J. Biochem. 122, 883-889 (1997)

Analysis of the Substrate Binding Site and Carboxyl Terminal Region of Vacuolar H$^+$-Pyrophosphatase of Mung Bean with Peptide Antibodies[1]

Ayako Takasu,* Yoichi Nakanishi,* Tokiko Yamauchi,* and Masayoshi Maeshima*,†,[2]

*Laboratory of Biochemistry, Graduate School of Bioagricultural Sciences, Nagoya University, Nagoya 464-01; and †Department of Cell Biology, National Institute for Basic Biology, Okazaki 444

Received for publication, June 30, 1997

Vacuolar H$^+$-translocating inorganic pyrophosphatase is a single-protein enzyme and uses a simple substance as an energy donor. Functional domains of the enzyme were investigated by using antibodies specific to peptides corresponding to the putative substrate-binding site (DVGADLVGKVE) in the hydrophilic loop and the carboxyl terminal part. The antibody to the former peptide clearly reacted with the pyrophosphatases of different plant species, and strongly inhibited the hydrolytic activity of the purified enzymes and the proton pumping activity of membrane vesicles. These results indicate that the sequence functions as an actual substrate-binding site and is a common motif. The antibody to the carboxyl terminal part reacted only to the mung bean enzyme, suppressing its hydrolytic and proton pumping activities. The results suggest that the carboxyl terminus is exposed to the cytosol and is close to the catalytic site. H$^+$-Pyrophosphatase hydrolyzed triphosphate and tetraphosphate at low rates. Phytic acid, *myo*-inositol hexaphosphate, inhibited the enzyme even in the presence of Mg^{2+}. The concentration for 50% inhibition was 0.15 mM. The inhibition of H$^+$-PPase by dicyclohexyldiimide was partly reversed by Mg^{2+}. The catalytic site and the membrane topology of the enzyme are discussed.

Key words: catalytic domain, H$^+$-pyrophosphatase, peptide antibody, proton pump, vacuole.

Vacuolar H$^+$-translocating inorganic pyrophosphatase is a unique proton pump with the following three characteristics. First, it consists of a single polypeptide with a molecular mass of about 80 kDa in a dimeric form (*1-7*), although the F- and V-type H$^+$-ATPases are composed of plural subunits. Second, the enzyme utilizes a simple, low cost substrate. PP_i is generated as a byproduct of several biosynthetic processes for macromolecules, such as protein, nucleic acids, and cellulose. Under normal conditions H$^+$-PPase has the capacity to pump H$^+$ into vacuoles against a pH gradient of 3 to 4 units (*8, 9*). Third, this highly efficient proton pump coexists with H$^+$-ATPase in a single vacuolar membrane (*8*). This property is related to the physiological function of H$^+$-PPase in plant cells. With respect to the first and second properties, H$^+$-PPase is a fine model for studying the coupling mechanism between the hydrolysis of a high energy phosphate bond and the translocation of protons. Vacuolar membrane PPase has been suggested to have the ability to pump K$^+$ ions into vacuoles (*1, 10*), although there is counterevidence (*11, 12*). Despite its importance in bioenergetics, however, the structure-function relationship of H$^+$-PPase has not yet been defined clearly.

H$^+$-PPase is widely distributed among higher plants, alga, and a photosynthetic bacterium, *Rhodospirillum rubrum* (*1, 7, 13-17*). The primary structures of H$^+$-PPase were deduced from the cDNAs of *Arabidopsis thaliana* (*3*), barley (*4*), sugar beet (*18*), tobacco (*19*), and rice (*20*). A few characteristic residues were determined. Kim *et al.* (*21*) reported that a sulfhydryl reagent, *N*-ethylmaleimide, covalently binds to Cys^{634} of *A. thaliana* H$^+$-PPase and thereby inhibits the enzyme. This residue is cytosolically oriented, and the inhibition by *N*-ethylmaleimide is prevented by the substrate and free Mg^{2+} (*22, 23*). *N,N'*-Dicyclohexylcarbodiimide (DCCD) also covalently binds to the H$^+$-PPase and thereby inhibits proton translocation (*2*). The H$^+$-PPase shares a consensus sequence with the DCCD binding subunits of F_oF_1-type and vacuolar-type H$^+$-ATPases (*4, 24*). Thus we speculate that DCCD reacts with a glutamate residue in the consensus sequence of barley H$^+$-PPase. Recently, Maruyama *et al.* (*25*) prepared peptide fragments of H$^+$-PPase by proteolytic digestion and determined that radiolabeled DCCD bound to a fragment of the membrane-spanning domain closest to the C-terminus.

From the sequence homology of H$^+$-PPase with soluble-type PPases, two sequences have been nominated as the catalytic site of H$^+$-PPase (*1, 26*). One of them, (E/D)-xxxxxxxKxE, is common among vacuolar H$^+$-PPases and is

[1] This work was supported by Grants-in-Aid for Scientific Research from the Ministry of Education, Science, Sports and Culture of Japan to M.M.

[2] To whom correspondence should be addressed. Tel: +81-52-789-4096, Fax: +81-52-789-4094, E-mail: maeshima@agr.nagoya-u.ac.jp

Abbreviations: DCCD, *N,N'*-dicyclohexylcarbodiimide; H$^+$-PPase, proton-translocating inorganic pyrophosphatase [EC 3.6.1.1]; KLH, keyhole limpet hemocyanin; M, membrane-spanning domain; PP_i, inorganic pyrophosphatase; PVDF, polyvinylidene difluoride.

deduced to be an essential functional sequence. We are conducting a series of experiments on H^+-PPase using mung bean hypocotyls as plant material, since a relatively high amount of the enzyme with high activity can be obtained from this tissue. Also we sequenced the cDNA for mung bean H^+-PPase (Nakanishi and Maeshima, unpublished data). In this study, we prepared an antibody to this sequence (DVGADLVGKVE) of mung bean H^+-PPase and examined its effect on the enzyme activity. Our observations confirmed the above deduction. An antibody to the C-terminal part was also prepared and used to study its orientation in the vacuolar membrane. Furthermore, we found that mung bean H^+-PPase catalyzed the hydrolysis of tri- and tetrapolyphosphates, which was strongly inhibited by *myo*-inositol hexaphosphate, phytic acid. Here, we discuss the catalytic site of the enzyme considering these results.

MATERIALS AND METHODS

Materials—Seeds of mung bean (*Vigna radiata* cv. Wilczek) were imbibed in 1 mM $CaSO_4$ and then germinated at 26°C for 3.5 d in the dark. Pyrophosphate, triphosphate, tetraphosphate, acridine orange, and phosphatidylcholine (soybean, type IV-S) were purchased from Sigma. Horseradish peroxidase-linked protein A was purchased from Amersham. All other products used were of analytical grade.

Vacuolar Membrane Preparation—Vacuolar membranes were prepared from hypocotyls of etiolated seedlings as described previously (*2*). All steps were carried out at 0-4°C, and the membranes were maintained on ice. Hypocotyls (300 g, fresh weight) were homogenized with a Polytron in 400 ml of cold homogenizing medium comprising 0.25 M sorbitol, 2 mM EGTA, 0.5 mM phenylmethylsulfonyl fluoride, 2 mM dithiothreitol, 1% (w/v) polyvinylpyrrolidone-40 (Sigma), and 50 mM Tris-acetate, pH 7.5. The homogenate was filtered and centrifuged 3,600 × *g* for 10 min. The supernatant was centrifuged at 120,000 × *g* for 30 min. The precipitate was suspended in 15 ml of 20 mM Tris-acetate, pH 7.5, 0.5 M sucrose, 1 mM EGTA, and 2 mM DTT, and then poured into a centrifugation tube. The suspension was overlaid with 10 ml of 20 mM Tris-acetate, pH 7.5, 0.25 M sorbitol, 1 mM EGTA, and 2 mM DTT. After centrifugation at 120,000 × *g* for 30 min, the interface portion was collected and diluted with the same volume of 20 mM Tris-acetate, pH 7.5, 0.25 M sorbitol, 1 mM EGTA, and 2 mM DTT. The suspension was centrifuged at 130,000 × *g* for 30 min, and then the resulting white pellet (vacuolar membranes) was suspended in 20 mM Tris-acetate, pH 7.5, 20% (w/v) glycerol, 2 mM DTT, 1 mM EGTA, and 20 mM $MgCl_2$ (Tris/GDEM). The protein content of the preparation was determined by the method of Bradford (*27*), and the membrane suspension was diluted to give a final concentration of 1.5 mg/ml. In some experiments, vacuolar membranes were prepared from thalli of *Conocephalum* (a moss), young leaves of *Kalanchoë* and tap roots of sugar beet, by the same method as for mung bean hypocotyls, and then used for immunoblotting (*13*).

Enzyme Purification—H^+-PPase was solubilized from membranes and purified by the method previously described (*2*) with a few modifications. Briefly, solid KCl and 10% (w/v) Triton X-100 were added to the membrane suspension at final concentrations of 50 mM and 0.2%, respectively, and then the suspension was centrifuged at 150,000 × *g* for 30 min. The pellet was suspended in Tris/GDEM containing 0.4% lysophosphatidylcholine to bring the volume to 0.5 of the original membrane suspension. The suspension was briefly sonicated, stirred at 25°C for 10 min, and then centrifuged at 150,000 × *g* for 40 min at 8°C. The supernatant was applied to a column (bed volume, 3 ml) of QAE-Toyopearl 550c preequilibrated with Tris/GDEM containing 0.1% Triton X-100 (Tris/GDEM/Triton). The column was washed with 10 ml of Tris/GDEM/Triton containing 50 mM NaCl, and then H^+-PPase was eluted from the column with 10 ml of Tris/GDEM/Triton containing 150 mM NaCl. Vacuolar H^+-ATPase was purified from mung bean hypocotyls as described previously (*28*).

Enzyme Assays—Enzyme activity was assayed as described previously (*2*). For H^+-PPase assays, L-α-phosphatidylcholine type IV-S was dissolved in 20 mM Tris-acetate, pH 7.5, and 2 mM DTT to give a final concentration of 2 mg/ml. PP_i hydrolysis measurements were carried out at 25°C in a reaction mixture comprising 1 mM sodium pyrophosphate, 1 mM $MgSO_4$, 50 mM KCl, 1 mM sodium molybdate, 0.02% Triton X-100, 20 μg of a phosphatidylcholine micelle suspension, and 30 mM Tris-Mes, pH 7.2. After incubation for 5-20 min at 30°C, the reaction was terminated, and the amount of P_i released was determined colorimetrically.

Proton Pumping Assays—Proton pumping by vacuolar membrane vesicles was monitored as acridine orange fluorescence quenching. The reaction mixture (2.2 ml) comprised 0.5 mM sodium PP_i, 0.25 M sorbitol, 25 mM Hepes/bistrispropane, pH 7.2, 50 mM KCl, and 1 μM acridine orange. Thirty micrograms of vacuolar membrane protein was typically used. The reaction was started at 25°C with 1 mM $MgSO_4$. Fluorescence quenching was monitored with a Shimadzu RF-5000 fluorescence spectrophotometer set at 493 nm for excitation and 540 nm for emission.

Gel Electrophoresis—SDS-PAGE in a 12% polyacrylamide gel was performed by the method of Laemmli (*29*). Samples were heated in 50 mM Tris-HCl, pH 6.8, 2% SDS, 20% glycerol, and 2% 2-mercaptoethanol at 70°C for 7 min prior to electrophoresis. Two-dimensional PAGE was carried out by the method of O'Farrell (*30*). Protein samples were suspended in 8 M urea, 2% Pharmalite (pH 4-6.5), 2.5% Triton X-100, 10 mM DTT, and 0.2% SDS. For gel analysis, samples were deposited on tube gels (2.5 mm, 8 cm) for IEF in the first dimension as described by O'Farrell (*30*). The second dimension was performed in a 12% polyacrylamide slab gel system with 0.1% SDS.

Immunoblot Analysis—Antibodies against subunits A and B of the mung bean vacuolar H^+-ATPase were prepared as described previously (*31*). For preparation of antibodies to peptides, the synthesized peptides were linked with keyhole limpet hemocyanin (KLH) using *m*-maleimidobenzoyl-*N*-hydroxysuccinimide ester (*32*). The conjugates were homogenized with Freund's complete adjuvant for the initial injection and Freund's incomplete adjuvant for the booster injections. The homogenates were injected into rabbits once a week for 5 consecutive weeks. IgG fractions were purified by Ampure PA (Amersham) column chromatography. For immunoblotting, proteins were separated

by SDS-PAGE and then transferred to a PVDF membrane (Millipore) with a semidry blotting apparatus by standard procedures (*33*). The membrane was blocked with 5% skim milk prior to reaction with the primary antibody. After rinsing, antibodies bound to the antigen were detected with horseradish peroxidase-coupled protein A and chemiluminescent reagents (Amersham).

RESULTS

Preparation of Peptide-Specific Antibodies—The vacuolar H⁺-PPase of mung bean is a single 80-kDa polypeptide composed of 766 amino acids (Nakanishi and Maeshima, unpublished data). Despite its simple structure, its functional domains have not yet been determined. The two configurations, $D(X)_4DXK(X)_4D$ and $(E/D)(X)_7KXE$, have been deduced to be catalytic sites of vacuolar H⁺-PPases, because these configurations are homologous to those of soluble-type PPases, such as yeast cytosolic PPase (*26*). The second motif is conserved as DVGADLVGKVE at position 253 of mung bean H⁺-PPase, but the first motif is not conserved in the mung bean enzyme. In order to determine whether the second motif is an actual catalytic site or not, we prepared antibodies against the peptide, DVGADLVGKVEC, conjugated with KLH protein. Also, to determine the location of the carboxyl terminal domain in the vacuolar membrane and its enzymatic significance, antibodies were prepared against the conjugate of KLH and the C-terminal sequence ATHGGLLFKIFC. Both antibodies clearly reacted with the mung bean H⁺-PPase (Fig. 1). The corresponding authentic peptide completely inhibited the immunochemical reaction in each antibody preparation, indicating the specificity of the antibodies. The antibodies to the putative substrate-binding site (DVGADLVGKVE) and the C-terminal domain (ATHGGLLFKIF) are referred to as antibody-S and antibody-C hereafter.

Immunoblotting with the Peptide Antibodies—Figure 2A shows immunoblots of H⁺-PPases prepared from different plant species with antibody-S and antibody-C. Antibody-S reacted with the H⁺-PPases from sugar beet, *Kalanchoë* (crassulacean acid metabolism plant), and *Conocephalum* (moss) in addition to the mung bean enzyme. The immunoreaction with the peptide-specific antibody suggests that the PPases of *Conocephalum, Kalanchoë*, and sugar beet contain the same sequence in their primary structures. Two isoforms of H⁺-PPase have been reported for sugar beet (*18*). Both isoforms contain the same sequences of putative substrate-binding sites as those of mung bean. Although the H⁺-PPase of *Acetabularia acetabulum* reacted with the antibody to the whole enzyme (*15*), antibody-S did not react with the H⁺-PPase of *A. acetabulum*. This suggests a slight difference in a few residues of the sequence.

In contrast, antibody-C only recognized mung bean H⁺-PPase, *i.e.* not the PPases from other plants. The absence of a reaction with antibody-C suggests a difference in their

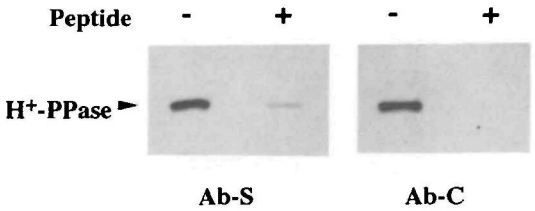

Fig. 1. **Specificity of antibodies to the putative substrate-binding site and the carboxyl-terminal domain of mung bean H⁺-PPase.** The purified mung bean H⁺-PPase (about 0.5 μg) was subjected to SDS-PAGE, and then transferred onto PVDF membranes. The membranes were immunostained with antibody-S (Ab-S) and antibody-C (Ab-C) in the presence or absence of the corresponding peptides (DVGADLVGKVEC for Ab-S, ATHGGLLFKIF for Ab-C) at the concentration of 2 μg/ml.

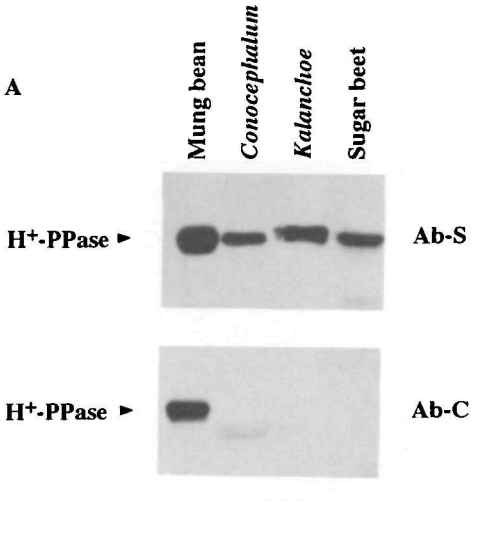

B

(a)

mung bean	Asp-Val-Gly-Ala-Asp-Leu-Val-Gly-Lys-Val-Glu
sugar beet	Asp-Val-Gly-Ala-Asp-Leu-Val-Gly-Lys-Val-Glu

(b)

mung bean	Ala-Thr-His-Gly-Gly-Leu-Leu-Phe-Lys-Ile-Phe
sugar beet	Ala-Thr-His-Gly-Gly-Leu-Leu-Phe-Lys- Leu-Phe
sugar beet	Ala-Thr-His-Gly-Gly-Leu-Leu-Phe-Lys- Tyr-Leu

Fig. 2. **Immunoblotting of the vacuolar H⁺-PPases of four plant species with antibody-S and antibody-C.** Vacuolar membranes were prepared from *Conocephalum, Kalanchoë* and sugar beet, and used for immunoblotting. A: Immunoblots with antibody-S (Ab-S) and antibody-C (Ab-C). In the case of antibody-C, incubation of the membrane filter with the antibody was performed in the presence of 1% Triton X-100. B: Comparison of the putative substrate-binding sites (a) and the carboxyl-terminal domains (b) of mung bean H⁺-PPase and sugar beet isoforms. The primary sequence of the sugar beet enzyme is cited from Kim *et al.* (*18*).

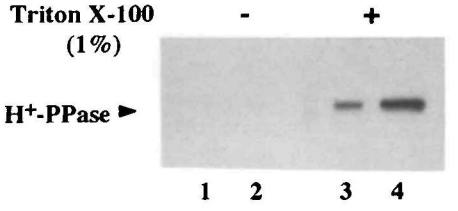

Fig. 3. **Effect of a detergent on the immunological reaction of antibody-C on immunoblotting.** The purified mung bean H⁺-PPase (lanes 1 and 3, 0.2 μg; lanes 2 and 4, 0.6 μg) was subjected to SDS-PAGE and then transferred onto a membrane filter. The membrane was incubated with the antibody solution in the presence (+) or absence (−) of 1% Triton X-100.

primary sequences in the carboxyl terminus. Indeed, one or two residues of the sugar beet H^+-PPase isoforms is different from in the mung bean enzyme. Note that the peptide antibodies recognize a difference in a single amino acid substitution.

Antibody-C could give an immunostained band on an immunoblot only in the presence of Triton X-100 in a reaction mixture containing the primary antibody (Fig. 3). These findings suggest that the C-terminus of mung bean H^+-PPase may face the hydrophobic interior space on the membrane filter in the absence of a detergent. Probably, Triton X-100 is necessary for exposure of the C-terminus to the solution.

The partially purified preparation of H^+-PPase was subjected to two-dimensional PAGE and immunoblot analysis to examine the presence of isoforms of the enzyme. As shown in Fig. 4, H^+-PPase gave a single spot with an isoelectric point of 5.9. While subunits A and B of mung bean H^+-ATPase gave two immunostained spots with different isoelectric points for each subunit (subunit A: pI, 5.7 and 5.6; subunit B: pI, 5.4 and 5.3). At the cDNA level, our previous data suggest the absence of isoforms of the H^+-PPase protein. Although there are two copies of the H^+-PPase gene in mung bean, the protein-coding regions of the two genes are identical. This indicates at the protein level the absence of isoforms of H^+-PPase in at least hypocotyl tissue.

Inhibition of Substrate Hydrolysis and Proton Translocation of H^+-PPase by the Peptide Antibodies—As discussed above, there may be a single species of H^+-PPase protein. Therefore, all the H^+-PPase of mung bean may react with the antibodies. If the corresponding site functions as a substrate-binding site, the activity may be reduced on binding with the antibody. Considering the control values, antibody-S inhibited H^+-PPase to 30% of the activities of PP_i hydrolysis and proton translocation (Fig. 5). The antibody molecules interact with the epitopes on the outer surface of the membrane vesicles. This indicates at least that the amino acid sequence, DVGADLVGKVE, faces the cytosolic side. Antibody-C also partially inhibited not only the PP_i-hydrolysis but also the proton pumping, suggesting that the C-terminal part faces the cytoplasmic side in the vacuoles.

Enzymatic Properties—Vacuolar H^+-PPase hydrolyzed triphosphate and tetraphosphate at relatively low rates as shown in Fig. 6. In the case of triphosphate, the first

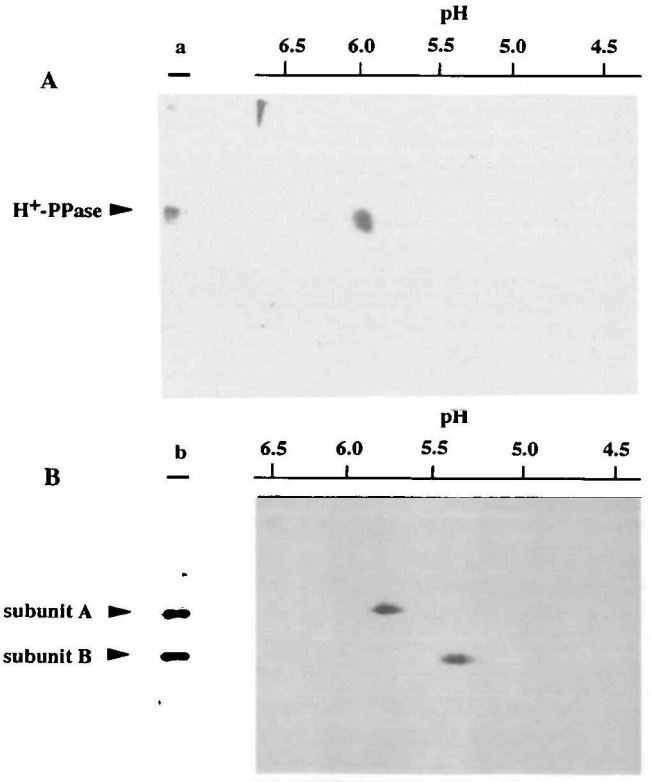

Fig. 4. **Two-dimensional PAGE of crude preparations of vacuolar H^+-ATPase and H^+-PPase, and immunoblotting with peptide antibodies.** The first and second electrophoreses comprised isoelectric focusing and SDS-PAGE, respectively. H^+-PPase (A) and H^+-ATPase (B) partially purified from mung bean vacuolar membranes were subjected to two-dimensional PAGE and immunoblotting. A: Immunoblot with antibody-S. B: Immunoblot with a mixture of antibodies against subunits A and B of mung bean vacuolar H^+-ATPase. Lanes a and b, the purified preparations of H^+-PPase and H^+-ATPase, respectively. Arrowheads indicate the subunits of the enzymes.

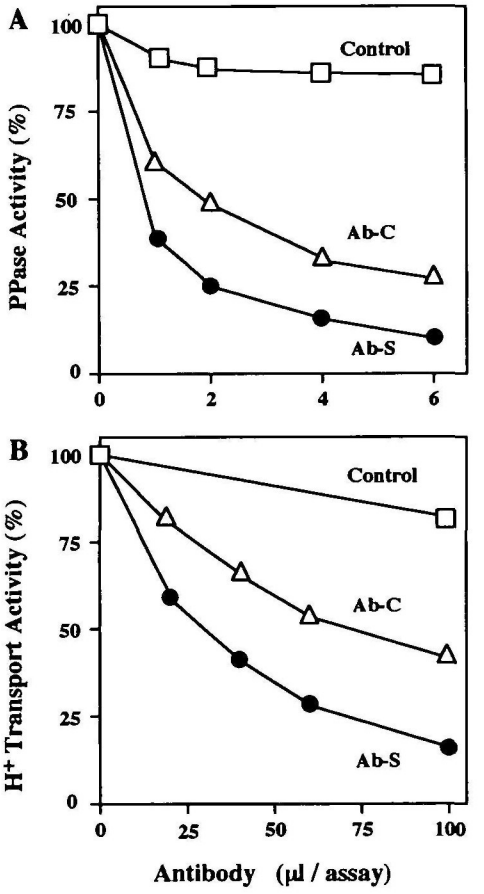

Fig. 5. **Effects of the peptide antibodies on the substrate hydrolysis and proton pumping of H^+-PPase.** A: The purified H^+-PPase (0.5 μg) was pre-incubated for 10 min at 25°C with the indicated amounts of antibody-S (5.0 mg/ml), antibody-C (7.0 mg/ml), or control IgG (7.0 mg/ml) prior to the addition of PP_i. The control activity of H^+-PPase was 4.0 μmol/min/mg. B: The vacuolar membrane vesicles (30 μg) were pre-incubated for 20 min at 25°C with the antibodies prior to the addition of PP_i. The control activity of PP_i-dependent pumping showed a 38% change in fluorescence/min.

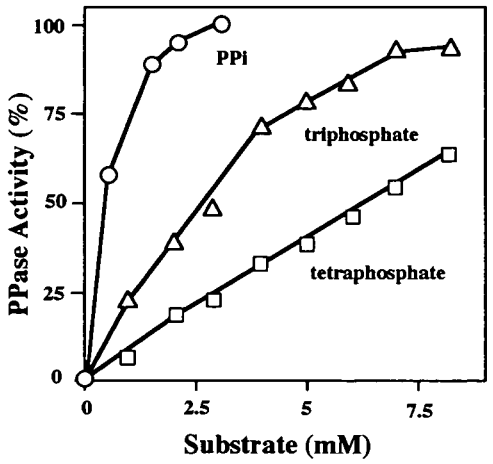

Fig. 6. **Substrate specificity of H⁺-PPase.** The assay medium for the purified H⁺-PPase contained PP_i, triphosphate or tetraphosphate at the indicated final concentrations. The concentrations of $MgCl_2$ in the reaction mixture were 1, 1.5, and 2.0 mM for PP_i, triphosphate and tetraphosphate, respectively. The control activity of H⁺-PPase for PP_i was 4.5 μmol/min/mg.

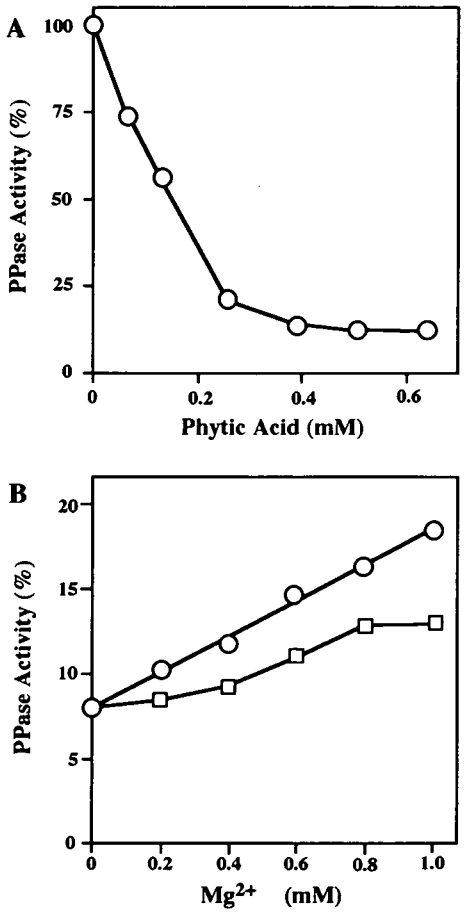

Fig. 7. **Inhibition of H⁺-PPase by phytic acid.** A: The purified H⁺-PPase was pre-incubated with phytic acid at the indicated concentrations at 0°C for 10 min, and then the enzyme activity was measured at 25°C for 10 min. The final concentration of $MgCl_2$ was 1.0 mM for each assay. B: The effect of Mg^{2+} on the H⁺-PPase inhibition by phytic acid. The enzyme was pre-incubated with phytic acid in the presence of Mg^{2+} at the indicated concentrations (open circles). The enzyme was pre-incubated with phytic acid in the absence of $MgCl_2$ (open squares). The control activity without phytic acid was 4.2 μmol/min/mg.

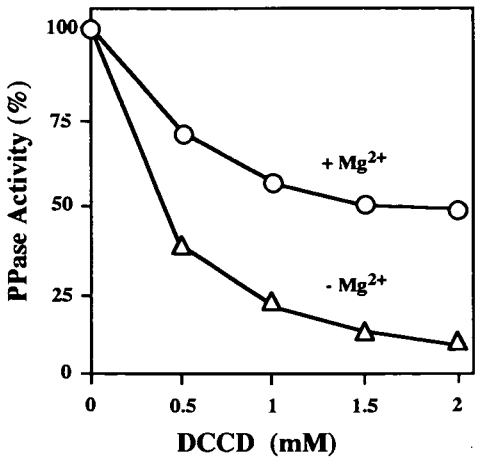

Fig. 8. **Effect of Mg^{2+} on the inhibition of H⁺-PPase by DCCD.** The purified H⁺-PPase was pre-incubated with DCCD at the indicated concentrations in the presence (open circles) or absence (open triangles) of 1 mM $MgCl_2$ at 0°C for 10 min. Then the enzyme activity was assayed at 25°C. DCCD was dissolved in methanol, and the solvent did not affect the enzyme activity at less than 5%.

reaction produces P_i and PP_i, and then in the second reaction PP_i is hydrolyzed quickly. Therefore, the amount of P_i in the reaction mixture is the total of the first and second reactions. The rate of the first reaction for triphosphate was calculated to be about 12% of the rate for PP_i. The hydrolysis of tri- and tetraphosphates by H⁺-PPase suggests that one side of pyrophosphate is relatively free in the catalytic pocket of the enzyme.

Figure 7A shows the inhibitory effect of phytic acid (*myo*-inositol hexaphosphate), a major store of phosphate in seeds. The concentration of phytic acid for half inhibition was about 150 μM. In seeds, phytic acid exists as a complex with magnesium and calcium ions. There is a possibility that phytic acid competes for Mg^{2+} with the H⁺-PPase. However, the activity was not recovered so extensively on the addition of Mg^{2+} to the pre-incubation medium. This suggests that the inhibition by phytic acid is due to the direct interaction of phytic acid with the enzyme molecule. Imidodiphosphate inhibited mung bean H⁺-PPase by only 50% at 1 mM even after pre-incubation for 10 min.

A potent inhibitor of proton transduction, DCCD, inhibited H⁺-PPase at high concentrations (Fig. 8). The inhibition by DCCD was partly reversed in the presence of Mg^{2+} at 1 mM. This is consistent with the previous observation of Maruyama *et al.* (*25*). As reported previously (*34, 35*), the H⁺-PPase has a binding site for free Mg^{2+}, and the binding of Mg^{2+} is essential for its enzymatic activity and functional structure. The present results suggest that Mg^{2+} binding to the enzyme molecule prevents the binding of DCCD.

DISCUSSION

Vacuolar H⁺-PPase is an attractive enzyme with a simple structure compared with other types of proton pumps. Information concerning its primary sequence has been accumulated with the cDNA cloning for vacuolar H⁺-PPases of *A. thaliana* (*3*), barley (*4*), sugar beet (*18*), tobacco (*19*), and rice (*20*). On comparison between H⁺-PPase and soluble PPases, Rea *et al.* (*26*) proposed that two

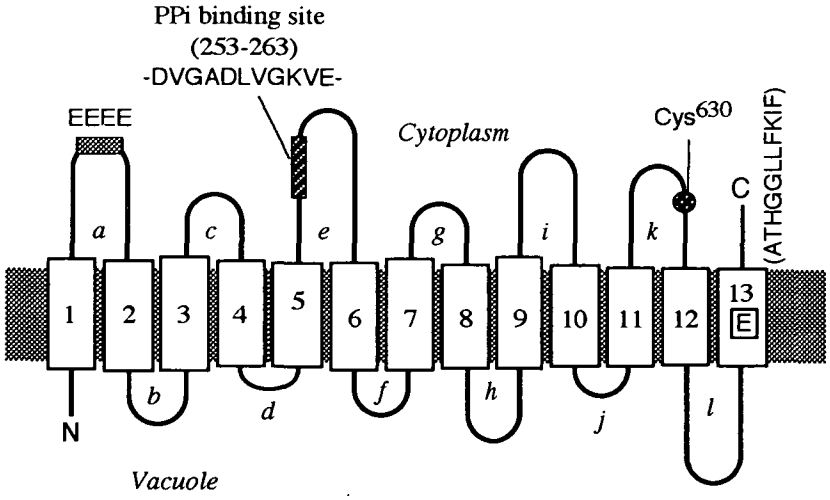

Fig. 9. **Hypothetical model of the membrane topology of vacuolar H⁺-PPase.** Thirteen membrane-spanning domains were predicted for mung bean H⁺-PPase (M1-M13). In our model, the putative substrate-binding site at position 253 is in cytosolic loop *e*, and the carboxyl terminal short part also faces the cytosol. The *N*-ethylmaleimide reactive Cys^{630} demonstrated previously (*21, 22*) is shown in cytosolic loop *k*. Maruyama *et al.* (*25*) demonstrated that DCCD binds to Glu 747 in M13.

motifs, DxxxxDxKxxxxD and (E/D)xxxxxxxKxE, are putative catalytic sites of H⁺-PPase. Although the first motif is not common to H⁺-PPase of mung bean, tobacco, beet, or barley, the second motif is conserved as the sequence, DVGADLVGKVE, among all H⁺-PPases except for that of *Arabidopsis* (DVGADLVGKIE). In this study, we prepared an antibody to the common sequence. The inhibitory effect of the antibody on both the activities of PP_i hydrolysis and proton pumping strongly indicates that the sequence is an actual substrate-binding site and is involved in the catalytic function in the cytoplasm. An antibody specific to the carboxyl terminal sequence consisting of 11 amino acids was also inhibitory toward enzymatic activity. Therefore, the carboxyl terminus is thought to face the cytosol.

In conclusion, we propose the schematic model of the membrane topology of H⁺-PPase shown in Fig. 9. The putative binding-site is in cytoplasmic loop *e*. There are ten negatively charged residues and five positively charged residues in loop *e*, and the net charge of the loop is negative. It is suitable for binding of the $MgPP_i$ complex and other free Mg^{2+} ions. Previously we proposed that the actual substrate for H⁺-PPase is $MgPP_i$ (*34*). More detailed investigations revealed that a substrate for the enzyme is Mg_2PP_i (*35-37*). Then a magnesium ion is essential for the stabilization and activation of H⁺-PPase (*23, 34-36*). The enzyme contains high- and low-affinity Mg^{2+}-binding sites with K_m values in the range of 20 to 42 μM and 0.25-0.45 mM, respectively. Cooperman *et al.* (*38*) deduced for a soluble type PPase, such as yeast cytosolic PPase, that the active site is filled with a PP_i molecule, three Mg^{2+} ions and a water molecule for PPase catalysis of PP_i hydrolysis. From the high affinity of the enzyme with Mg^{2+}, we speculate that the active site pocket is highly negatively charged. Thus, cytoplasmic loop *e* containing the DVGADLGKVE sequence is a good candidate for the main chain of the active site. Probably, several cytosolic loops including loops *e* and *k* comprise the tertiary structure of the catalytic part. The C-terminal part may be close to the catalytic site, and the antibody binding to this segment may cause steric hindrance of PP_i catalysis by the enzyme. The C-terminal part seems to be more important for the function than the N-terminal part, because the sequence homology of the C-terminal part (90%) among various H⁺-PPases is higher than that of the N-terminal part (less than 40%).

To clarify the functional domain and catalytic residues of H⁺-PPase by site-directed mutagenesis, we must establish an expression system in *Escherichia coli* or yeast. A successful attempt has been reported by Kim *et al.* (*21*). In addition to molecular genetic approaches, direct observation of the tertiary structure of the enzyme protein is also expected. Recently, Heikinheimo *et al.* (*39*) reported the high-resolution structure of yeast soluble PPase. Fortunately, plant vacuolar membranes of young tissues contain a relatively high amount of H⁺-PPase, *i.e.* about 10% of the total membrane protein (*2*). We must obtain two-dimensional crystals of H⁺-PPase, as reported for aquaporin (*40*), and three-dimensional crystals using fragments of specific antibodies as reported for cytochrome *c* oxidase (*41*). The antibodies prepared in this study may be useful for the preparation of such crystals.

REFERENCES

1. Rea, P.A. and Poole, R.J. (1993) Vacuolar H⁺-translocating pyrophosphatase. *Annu. Rev. Plant Physiol. Plant Mol. Biol.* **44**, 157-180
2. Maeshima, M. and Yoshida, S. (1989) Purification and properties of vacuolar membrane proton-translocating inorganic pyrophosphatase from mung bean. *J. Biol. Chem.* **264**, 20068-20073
3. Sarafian, V., Kim, Y., Poole, R.J., and Rea, P.A. (1992) Molecular cloning and sequence of cDNA encoding the pyrophosphate-energized vacuolar membrane proton pump (H⁺-PPase) of *Arabidopsis thaliana*. *Proc. Natl. Acad. Sci. USA* **89**, 1775-1779
4. Tanaka, Y., Chiba, K., Maeda, M., and Maeshima, M. (1993) Molecular cloning of cDNA for vacuolar membrane proton-translocating inorganic pyrophosphatase in *Hordeum vulgare*. *Biochem. Biophys. Res. Commun.* **190**, 1110-1114
5. Maeshima, M. (1990) Oligomeric structure of H⁺-translocating inorganic pyrophosphatase of plant vacuoles. *Biochem. Biophys. Res. Commun.* **168**, 1157-1162
6. Sato, M.H., Maeshima, M., Ohsumi, Y., and Yoshida, M. (1991) Dimeric structure of H⁺-translocating pyrophosphatase from pumpkin vacuolar membranes. *FEBS Lett.* **290**, 177-180
7. Becker, A., Canut, H., Lüttge, U., Maeshima, M., Marigo, G., and Ratajczak, R. (1995) Purification and immunological comparison of the tonoplast H⁺-pyrophosphatase from cells of *Catharanthus roseus* and leaves from *Mesembryanthemum crystallinum* performing C_3-photosynthesis and the obligate CAM-plant *Kalan-*

choë daigremontiana. J. Plant Physiol. **146**, 88-94
8. Hedrich, R., Kurkdjian, A., Guern, J., and Flügge, U.I. (1989) Comparative studies on the electrical properties of the H⁺ translocating ATPase and pyrophosphatase of the vacuolar-lysosomal compartment. *EMBO J.* **8**, 2835-2841
9. Davies, J.M., Poole, R.J., and Sanders, D. (1993) The computed free energy change of hydrolysis of inorganic pyrophosphate and ATP: apparent significance for inorganic-pyrophosphate-driven reactions of intermediary metabolism. *Biochim. Biophys. Acta* **1141**, 29-36
10. Davies, J.M., Poole, R.J., Rea, P.A., and Sanders, D. (1992) Potassium transport into plant vacuoles energized directly by a proton-pumping inorganic pyrophosphatase. *Proc. Natl. Acad. Sci. USA* **89**, 11701-11705
11. Sato, M.H., Kasahara, M., Ishii, N., Homareda, H., Matsui, H., and Yoshida, M. (1994) Purified vacuolar inorganic pyrophosphatase consisting of a 75-kDa polypeptide can pump H⁺ into reconstituted proteoliposomes. *J. Biol. Chem.* **269**, 6725-6728
12. Ros, R., Romieu, C., Gibrat, R., and Grignon, C. (1995) The plant inorganic pyrophosphatase does not transport K⁺ in vacuole membrane vesicles multilabeled with fluorescent probes for H⁺, K⁺, and membrane potential. *J. Biol. Chem.* **270**, 4368-4374
13. Maeshima, M., Mimura, T., and Sato, T. (1994) Distribution of vacuolar H⁺-pyrophosphatase and a membrane integral protein in a variety of green plants. *Plant Cell Physiol.* **35**, 323-328
14. Takeshige, K., Tazawa, M., and Hager, A. (1988) Characterization of the H⁺-translocating adenosine triphosphatase and pyrophosphatase of vacuolar membranes isolated by means of a perfusion technique from *Chara corallina. Plant Physiol.* **86**, 1168-1173
15. Ikeda, M., Satoh, S., Maeshima, M., Mukohata, Y., and Moritani, C. (1991) A vacuolar ATPase and pyrophosphatase in *Acetabularia acetabulum. Biochim. Biophys. Acta* **1070**, 77-82
16. Nore, B.F., Sakai-Nore, Y., Maeshima, M., Baltscheffsky, M., and Nyrén, P. (1991) Immunological cross-reactivity between proton-pumping inorganic pyrophosphatases of widely phylogenic separated species. *Biochem. Biophys. Res. Commun.* **181**, 962-967
17. Nyrén, P., Nore, B.F., and Strid, A. (1991) Proton-pumping *N,N′*-dicyclohexylcarbodiimide-sensitive inorganic pyrophosphate synthase from *Rhodospirillum rubrum*: purification, characterization, and reconstitution. *Biochemistry* **30**, 2883-2887
18. Kim, Y., Kim, E.J., and Rea, P.A. (1994) Isolation and characterization of cDNAs encoding the vacuolar H⁺-pyrophosphatase of *Beta vulgaris. Plant Physiol.* **106**, 375-382
19. Lerchl, J., König, S., Zrenner, R., and Sonnewald, U. (1995) Molecular cloning, characterization and expression analysis of isoforms encoding tonoplast-bound proton-translocating inorganic pyrophosphatase in tobacco. *Plant Mol. Biol.* **29**, 833-840
20. Sakakibara, Y., Kobayashi, H., and Kasamo, K. (1996) Isolation and characterization of cDNAs encoding vacuolar H⁺-pyrophosphates isoforms from rice (*Oryza sativa* L.). *Plant Mol. Biol.* **31**, 1029-1038
21. Kim, E.J., Zhen, R.-G., and Rea, P.A. (1995) Site-directed mutagenesis of vacuolar H⁺-pyrophosphatase: necessity of Cys^{634} for inhibition by maleimides but not catalysis. *J. Biol. Chem.* **270**, 2630-2635
22. Zhen, R.-G., Kim, E.J., and Rea, P.A. (1994) Localization of cytosolically orientated maleimide-reactive domain of vacuolar H⁺-pyrophosphatase. *J. Biol. Chem.* **269**, 23342-23350
23. Gordon-Weeks, R., Steele, S.H., and Leigh, R.A. (1996) The role of magnesium, pyrophosphate, and their complexes as substrates and activators of the vacuolar H⁺-pumping inorganic pyrophosphatase. *Plant Physiol.* **111**, 195-202
24. Nyrén, P., Sakai-Nore, Y., and Strid, A. (1993) Amino acid sequence similarities between the vacuolar proton-pumping inorganic pyrophosphatase and the c-subunit of F_oF_1-ATPases. *Plant Cell Physiol.* **34**, 375-378
25. Maruyama, C., Sato, M.H., and Yoshida, M. (1994) Analysis of plant vacuolar H⁺-pyrophosphates by chemical modification (in Japanese). *Seikagaku* **66**, 709
26. Rea, P.A., Kim, Y., Sarafian, V., Poole, R.J., Davies, J.M., and Sanders, D. (1992) Vacuolar H⁺-translocating pyrophosphatases: a new category of ion translocase. *Trends Biochem. Sci.* **17**, 348-353
27. Bradford, M.M. (1976) A rapid and sensitive method for the quantitation of microgram quantities of protein utilizing the principle of protein-dye binding. *Anal. Biochem.* **72**, 248-254
28. Matsuura-Endo, C., Maeshima, M., and Yoshida, S. (1990) Subunit composition of vacuolar membrane H⁺-ATPase from mung bean. *Eur. J. Biochem.* **187**, 745-751
29. Laemmli, U.K. (1970) Cleavage of structural proteins during the assembly of the head of bacteriophage T_4. *Nature* **277**, 680-685
30. O'Farrell, P.H. (1975) High-resolution two-dimensional electrophoresis of proteins. *J. Biol. Chem.* **250**, 4007-4021
31. Matsuura-Endo, C., Maeshima, M., and Yoshida, S. (1992) Mechanism of the decline in vacuolar H⁺-ATPase activity in mung bean hypocotyls during chilling. *Plant Physiol.* **100**, 718-722
32. Liu, F.-T., Zinnecker, M., Hamaoka, T., and Katz, D.H. (1979) New procedures for preparation and isolation of conjugates of proteins and a synthetic copolymer of D-amino acids and immunochemical characterization of such conjugates. *Biochemistry* **18**, 690-697
33. Harlow, E. and Lane, D. (1988) *Antibodies: A Laboratory Manual*, pp. 471-510, Cold Spring Harbor Laboratory Press, Cold Spring Harbor, NY
34. Leigh, R.A., Pope, A.J., Jennings, I.R., and Sanders, D. (1992) Kinetics of the vacuolar H⁺-pyrophosphatase from higher plants: the role of magnesium, pyrophosphate, and their complexes as substrates, activators, and inhibitors. *Plant Physiol.* **100**, 1689-1705
35. Maeshima, M. (1991) H⁺-translocating inorganic pyrophosphatase of plant vacuoles: inhibition by Ca^{2+}, stabilization by Mg^{2+} and immunological comparison with other inorganic pyrophosphatases. *Eur. J. Biochem.* **196**, 11-17
36. Baykov, A.A., Bakuleva, N.P., and Rea, P.A. (1993) Steady-state kinetics of substrate hydrolysis by vacuolar H⁺-pyrophosphatase: A simple three-state model. *Eur. J. Biochem.* **217**, 755-762
37. Baykov, A.A., Sergina, N.V., Evtushenko, O.A., and Dubnova, E.B. (1996) Kinetic characterization of the hydrolytic activity of the H⁺-pyrophosphatase of *Rhodospirillum rubrum* in membrane-bound and isolated states. *Eur. J. Biochem.* **236**, 121-127
38. Cooperman, B.S., Baykov, A.A., and Lahti, R. (1992) Evolutionary conservation of the active site of soluble inorganic pyrophosphatase. *Trends Biochem. Sci.* **17**, 262-266
39. Heikinheimo, P., Lehtonen, J., Baykov, A., Lahti, R., Cooperman, B.S., and Goldman, A. (1996) The structural basis for pyrophosphatase catalysis. *Structure* **4**, 1491-1508
40. Walz, T., Hirai, T., Murata, K., Heymann, J.B., Mitsuoka, K., Fujiyoshi, Y., Smith, B.L., Agre, P., and Engel, A. (1997) The three-dimensional structure of aquaporin-1. *Nature* **387**, 624-627
41. Iwata, S., Ostermeier, C., Ludwig, B., and Michel, H. (1995) Structure at 2.8 Å resolution of cytochrome *c* oxidase from *Paracoccus denitrificans. Nature* **376**, 660-669